AMERICAN SOCIETY FOR MICROBIOLOGY | Antimicrobial Agents and Chemotherapy

Dissecting the Structure-Function Relationship of a Fungicidal Peptide Derived from the Constant Region of Human Immunoglobulins

Tecla Ciociola,[a] Thelma A. Pertinhez,[b]* Laura Giovati,[a] Martina Sperindè,[a] Walter Magliani,[a] Elena Ferrari,[c] Rita Gatti,[d] Tiziana D'Adda,[e] Alberto Spisni,[f] Stefania Conti,[a] Luciano Polonelli[a]

Units of Microbiology and Virology,[a] Biochemistry,[c] Anatomy, Histology and Embryology,[d] and Pathologic Anatomy,[e] Department of Biomedical, Biotechnological and Translational Sciences, University of Parma, Parma, Italy; CIM Laboratory, Technopole Parma, University of Parma, Parma, Italy[b]; Department of Surgical Sciences, University of Parma, Parma, Italy[f]

Synthetic peptides encompassing sequences related to the complementarity-determining regions of antibodies or derived from their constant region (Fc peptides) were proven to exert differential antimicrobial, antiviral, antitumor, and/or immunomodulatory activities *in vitro* and/or *in vivo*, regardless of the specificity and isotype of the parental antibody. Alanine substitution derivatives of these peptides exhibited unaltered, increased, or decreased candidacidal activities *in vitro*. The bioactive IgG-derived Fc N10K peptide (NQVSLTCLVK) spontaneously self-assembles, a feature previously recognized as relevant for the therapeutic activity of another antibody-derived peptide. We evaluated the contribution of each residue to the peptide self-assembling capability by circular-dichroism spectroscopy. The interaction of the N10K peptide and its derivatives with *Candida albicans* cells was studied by confocal, transmission, and scanning electron microscopy. The apoptosis and autophagy induction profiles in yeast cells treated with the peptides were evaluated by flow cytometry, and the therapeutic efficacy against candidal infection was studied in a *Galleria mellonella* model. Overall, the results indicate a critical role for some residues in the self-assembly process and a correlation of that capability with the candidacidal activities of the peptides *in vitro* and their therapeutic effects *in vivo*.

Infections are a major concern for public health, mainly due to multidrug-resistant and emerging or reemerging pathogens. Although antibiotics have been among the most significant contributions of modern science, leading to an increase in average lifetime expectancy, their effectiveness has been declining over time. Researchers are constantly looking for alternative anti-infective strategies, e.g., phage therapy, and new classes of drugs endowed with different mechanisms of action, such as peptides, phytochemicals, metalloantibiotics, lipopolysaccharides, and efflux pump inhibitors (1). In this context, our research group has been studying the anti-infective potential of synthetic peptides corresponding to antibody (Ab) fragments (2, 3). In previous studies, it was demonstrated that irrespective of the specificity of the native Ab for a given antigen, peptides related to Ab complementarity-determining regions may exert differential *in vitro*, *ex vivo*, and *in vivo* antimicrobial, antiviral, antitumor, and immunomodulatory activities (4–8). Similarly, synthetic peptides representing fragments of the constant region of Abs (Fc peptides) were also reported to display fungicidal and/or immunomodulatory activities *in vitro* and/or *in vivo*, regardless of the isotype of the relevant Ab (9, 10). In particular, the IgG1-derived Fc N10K peptide (NQVSLTCLVK) turned out to be active *in vitro* at micromolar concentrations against several fungi, including multidrug-resistant strains, and protected mice against experimental systemic and mucosal candidiasis, being devoid of hemolytic, cytotoxic, and genotoxic effects. In addition, circular-dichroism (CD) studies proved that the N10K peptide self-aggregates, forming β-sheet structures in few hours after solution, and electron micrographs confirmed the presence of a network of fibril-like structures (9). These and previous studies pointed to a possible correlation between the self-aggregation property of bioactive peptides and *in vivo* therapeutic efficacy (11). Alanine substitution derivatives (ASDs) of the N10K peptide, obtained by the replacement of each amino acid with alanine, revealed variable anti-*Candida* activities *in vitro* (9).

Here we present the results of further studies on the N10K peptide and N10K peptide ASDs aimed to give an answer to the importance of self-aggregation in defining their candidacidal activities *in vitro* and *in vivo*. We found a critical role played by some residues in the process of self-aggregation and verified that indeed self-aggregation affects the candidacidal activities of ASDs *in vitro* and their therapeutic effects *in vivo*. These results provide useful hints for the design of new and more effective antimicrobial peptides.

MATERIALS AND METHODS

Peptide synthesis. IgG1-derived Fc N10K peptide (NQVSLTCLVK) and its ASDs, defined according to the position of the amino acid replaced with alanine (Table 1), were synthesized using the fluoren-9-ylmethoxycarbonyl (Fmoc) solid-phase synthesis chemistry on a Syro II peptide synthesizer (MultiSynTech, Germany) at CRIBI Peptide Facility (Univer-

Received 21 July 2015 **Returned for modification** 5 September 2015
Accepted 3 February 2016

Accepted manuscript posted online 8 February 2016

Citation Ciociola T, Pertinhez TA, Giovati L, Sperindè M, Magliani W, Ferrari E, Gatti R, D'Adda T, Spisni A, Conti S, Polonelli L. 2016. Dissecting the structure-function relationship of a fungicidal peptide derived from the constant region of human immunoglobulins. Antimicrob Agents Chemother 60:2435–2442. doi:10.1128/AAC.01753-15.

Address correspondence to Stefania Conti, stefania.conti@unipr.it.

* Present address: Thelma A. Pertinhez, Transfusion Medicine Unit, Arcispedale Santa Maria Nuova—IRCCS, Reggio Emilia, Italy.

T.C. and T.A.P. contributed equally to this article.

Supplemental material for this article may be found at http://dx.doi.org/10.1128/AAC.01753-15.

TABLE 1 Amino acid sequences and properties of N10K and alanine substitution derivatives

Peptide	Sequence[a]	Candidacidal activity[b]	[θ][c]
N10K parental peptide	NQVSLTCLVK		31.72
ASDs			
N1A	**A**QVSLTCLVK	0.58	194.39
Q2A	N**A**VSLTCLVK	2.30	−23.57
V3A	NQ**A**SLTCLVK	5.91	−22.03
S4A	NQV**A**LTCLVK	2.38	154.05
L5A	NQVS**A**TCLVK	0.88	−37.11
T6A	NQVSL**A**CLVK	4.86	14.92
C7A	NQVSLT**A**LVK	54.66	77.23
L8A	NQVSLTC**A**VK	0.74	−25.64
V9A	NQVSLTCL**A**K	1.77	−24.91
K10A	NQVSLTCLV**A**	ND[d]	ND

[a] The alanine substitution is in bold.
[b] EC_{50} of ASD/EC_{50} of N10K peptide (9).
[c] Molar mean residue ellipticity [θ], 10^3 (degrees square centimeter per decimole), at 200 nm.
[d] ND, not determined (peptide not soluble).

sity of Padua, Italy). Crude peptides were purified by preparative reverse-phase high-performance liquid chromatography (HPLC) with a C_{18} column. Molecular masses of the peptides were confirmed by mass spectroscopy on a matrix-assisted laser desorption ionization–time of flight (MALDI TOF/TOF) mass spectrometer (model 4800; Applied Biosystems). The purity of the peptides was in the range of 80 to 90% as evaluated by analytical reverse-phase HPLC. Net peptide content was determined by an HP Amino Quant series II 1090L amino acid analyzer connected to an HP Kayak PIII personal computer (500 MHz; Centro Grandi Strumenti, University of Pavia, Italy).

Circular-dichroism spectroscopy. CD measurements were obtained on a Jasco 715 spectropolarimeter (Jasco International Co. Ltd., Japan) coupled to a Peltier PTC-348WI system for temperature control. Far-UV spectra were recorded at 20°C in the range of 250 to 190 nm in 0.5-nm-wavelength steps at a 50-nm/min scanning speed, at a 1.0-nm bandwidth with 4 accumulations, using a 1-mm-path-length quartz cuvette. Peptides (diluted to a final concentration of 100 μM) were analyzed immediately or at different time points (24 and 72 h, 7 days, or several months) after preparation of the starting aqueous solution (900 μM), to monitor the aggregation process. The spectra were water baseline corrected, and the spectral intensity was converted to molar mean residue ellipticity [θ] (degrees square centimeter per decimole). Kinetics of dissociation of selected peptides was evaluated upon dilution at 50 μM as a function of time, and the data were fitted to a single exponential curve. The fitting constant *k* corresponds to the dissociation rate constant. Thermal disaggregation of the N10K peptide was monitored at 200 nm from 20°C to 90°C with a temperature increase of 1°C/min, in the absence or presence of 500 μM laminarin, a soluble form of the β-1,3-glucans naturally occurring in the *Candida albicans* cell wall. Under both conditions, a whole spectrum was acquired at 20°C, at 90°C, and after cooling back at 20°C, to evaluate the reversibility of the process. Selected N10K peptide ASDs were also analyzed at 100 μM in the presence of 500 μM laminarin or at 900 μM in the presence of *C. albicans* SC5314 (5×10^7 cells/ml) using a 0.1-mm-path-length cuvette.

Time kinetics of peptide-mediated killing of *C. albicans*. The *in vitro* activities of the N10K peptide and selected ASDs against *C. albicans* SC5314 were evaluated at different times (30, 60, 120, 240, and 360 min) by CFU assays as previously described (9). The selected peptides were used at their minimal fungicidal concentrations, previously assessed by CFU assays. Each CFU assay was performed in triplicate. The activity was expressed as percent killing, calculated as 100 − (average number of CFU in the peptide-treated group/average number of CFU in the control group) × 100. Reported data represent the averages from three independent experiments.

Labeling of peptides with FITC. Fluorescein isothiocyanate (FITC) was dissolved in anhydrous dimethyl sulfoxide at a concentration of 1 mg/ml immediately before use. With gentle stirring, aliquots of 5 μl were added to each peptide (1.8 mM in 0.1 M sodium carbonate, pH 9), using a molar ratio of FITC to peptide of 1:1. The reaction mixture was kept at 4°C in the dark for 8 h, then NH_4Cl was added to a final concentration of 50 mM, and incubation was continued overnight at 4°C. Labeled peptides were separated by reverse-phase chromatography using an ÄKTA purifier system and a SOURCE 15RPC ST 4.6/100 column (GE Healthcare). Briefly, each completed labeling reaction mixture was loaded under acidic conditions (0.065% trifluoroacetic acid) and eluted in an acetonitrile gradient containing 0.050% trifluoroacetic acid. During elution, the optical absorbances at 495 and 215 nm were monitored in order to select peptide-containing fractions and to calculate the peptide concentration. After lyophilization, the powders of each fraction were dissolved in dimethyl sulfoxide, then diluted in sterile water to a proper concentration, and assayed for candidacidal activity as previously described (9). Active fractions were stored at 4°C until use.

Confocal microscopy studies. Interaction between *C. albicans* SC5314 cells and labeled peptides was monitored in time-lapse by a confocal microscope (LSM 510 Meta scan head integrated with an Axiovert 200 M inverted microscope; Carl Zeiss, Jena, Germany). Yeast cells from an aqueous colony grown on Sabouraud dextrose agar (SDA) for 24 h were suspended in 10 ml of yeast extract, peptone, and dextrose broth and incubated overnight at 30°C with shaking (100 rpm). Twenty microliters from a suspension of 2×10^7 cells/ml was seeded on coverslips mounted in a special flow chamber (12). A selected field was kept and observed during the time-lapse experiment. After 30 min, the labeled peptide was added (final concentration 180 μM). Images were taken thereafter every 15 min for up to 3 h. Propidium iodide, a nonvital nuclear stain commonly used for identifying dead cells, was added (1.5 μM) after 30 min. Samples were observed through a 63× numerical aperture (NA) 1.4 plan apo oil objective. Propidium iodide and FITC were excited with 543-nm He-Ne and 488-nm argon laser lines, respectively. Acquisition was carried out in a multitrack mode (namely, through consecutive and independent optical pathways).

Candidacidal activities of the peptides under the adopted conditions were verified as described above.

Evaluation of apoptosis and autophagy induction profiles in *C. albicans* after treatment with selected peptides. Peptide-induced apoptosis and autophagy in *C. albicans* SC5314 cells were evaluated by the Muse cell analyzer (Merck Millipore, Germany). The potential apoptotic effect was assessed using the Muse annexin V and dead cell assay kit, based on the detection of phosphatidylserine on the surface of apoptotic cells, while autophagy was assessed by the Muse autophagy LC3 antibody-based kit, designed to measure endogenous levels of LC3. Yeast cells from a colony grown on SDA for 24 h were suspended in water (5×10^5 cells/ml), in the presence or absence (control) of selected peptides at their previously established (9) half-maximal effective concentration (EC_{50}) or at 2× EC_{50}, for 30 min and 120 min. For the evaluation of the apoptotic profile, 20 min before the measurements, 90 μl each of treated and control cell suspensions were added to 10 μl of 10% bovine serum albumin and 100 μl of Muse annexin V and dead cell assay reagent, maintaining the mixture at room temperature in the dark. For the evaluation of the autophagy induction profile, after 30 min, 200 μl each of treated and control cell suspensions were centrifuged, and the pellets were resuspended in 200 μl of water plus 0.2 μl of autophagy reagent A and incubated for 2 h at 37°C. Subsequently, after centrifugation and washing, 5 μl of anti-LC3 fluorescent antibody and 95 μl of autophagy reagent B were added to the cells and then incubated on ice for 30 min in the dark. Cells were then washed with assay buffer and resuspended in 200 μl of the same buffer prior to data

acquisition. Data were acquired according to the manufacturer's instructions.

TEM studies. Aliquots (5 μl) of selected peptides at different concentrations (450, 100, 50, 10, 5, 1, and 0.59 μM), obtained immediately or at different time points (up to several months) after preparation of the starting solution, were applied to 200-mesh Formvar-coated copper grids and allowed to stand 1 min. After careful removal of the excess solvent by capillary action with filter paper, a filtered solution of 2% (wt/vol) uranyl acetate in water (5 μl for 1 min) was applied for negative staining. Excess stain was removed and the grids were air dried prior to examination in a Philips EM 208S transmission electron microscope (Fei Europe, Eindhoven, The Netherlands) operating at an accelerating voltage of 80 kV. For transmission electron microscopy (TEM) studies involving yeasts, germinating cells were obtained by inoculating 1 ml of the broth culture, prepared as previously described, in 10 ml of medium 199 and then incubated for 90 min at 37°C with shaking (150 rpm). Aliquots of *C. albicans* suspensions (2×10^7 cells/ml) containing equal numbers of budding and germinating cells in the absence (control) or presence of selected peptides were applied to grids and stained as previously described.

Scanning electron microscopy (SEM) studies. Yeast cell suspensions prepared as previously described were incubated in the presence or absence (control) of selected peptides (225 μM) for 60 min. After incubation, cell suspensions, placed on 25-mm^2 glass slides, were fixed with 2.5% glutaraldehyde in sodium cacodylate buffer 0.1 M, pH 7.4, and maintained at 4°C. Slides were washed in sodium cacodylate buffer for about 30 min and dehydrated by immersion in alcohol solutions in a 25 to 100% gradient (10 to 20 min for 25, 50, and 75% solutions and 30 to 40 min for 90 and 100% solutions). Subsequently, samples were washed in 100% acetone and dried in liquid CO_2 (31.1°C and 72.9 atm). Finally, slides were fixed on a support, gold coated in an ion-sputtering unit, and observed in a Philips 501 scanning electron microscope (15 kV). At the same time, properly diluted cell suspensions were plated on SDA to verify, by a conventional CFU assay, the candidacidal activities of the peptides under the adopted conditions (9).

Evaluation of *in vivo* toxicities and therapeutic activities of selected peptides. *In vivo* toxicities and potential therapeutic effects of selected peptides were studied in the *Galleria mellonella* model (13). To evaluate peptide toxicity, groups of 16 larvae at their final instar stage (body weight, 450 ± 20 mg) were inoculated (10 μl/larva) directly in the hemocoel, via the last left proleg, with the selected peptides (10 μmol/kg). Control groups consisted of larvae untouched or inoculated with 10 μl of saline solution. Larvae were then transferred to clean petri dishes (one for each experimental group), incubated at 37°C in the dark for 9 days, and scored daily for survival.

Potential therapeutic activities of selected peptides were evaluated by inoculating 10 μl of a *C. albicans* SC5314 suspension (5×10^5 cells/larva) via the last left proleg. Thirty minutes after *Candida* infection, larvae (16/group) were injected via the last right proleg (single injection of 10 μl) with the selected peptides (10 μmol/kg) or saline (control). Larval survival was monitored daily for up to 9 days after infection. Survival curves of peptide-treated and control animals were compared by the Mantel-Cox log rank test. A P value of <0.05 was considered significant.

RESULTS

ASD peptide conformational state. To evaluate the contribution of each residue to the self-assembly process, CD spectra of all ASDs in aqueous solution were acquired at 0, 24, and 72 h after solution, with the exception of the K10A ASD, which, as expected, was not soluble. Like the N10K peptide, at time zero the majority of ASDs presented a typical random coil conformation; the S4A and C7A ASDs, instead, showed straightaway a well-defined β-sheet structural organization (Fig. 1A). Over time, based on the appearance of two dichroic bands at 200 nm and 218 nm, a structural evolution to β-sheet organized structures was observed for the N10K peptide and the T6A and N1A ASDs. In particular, the

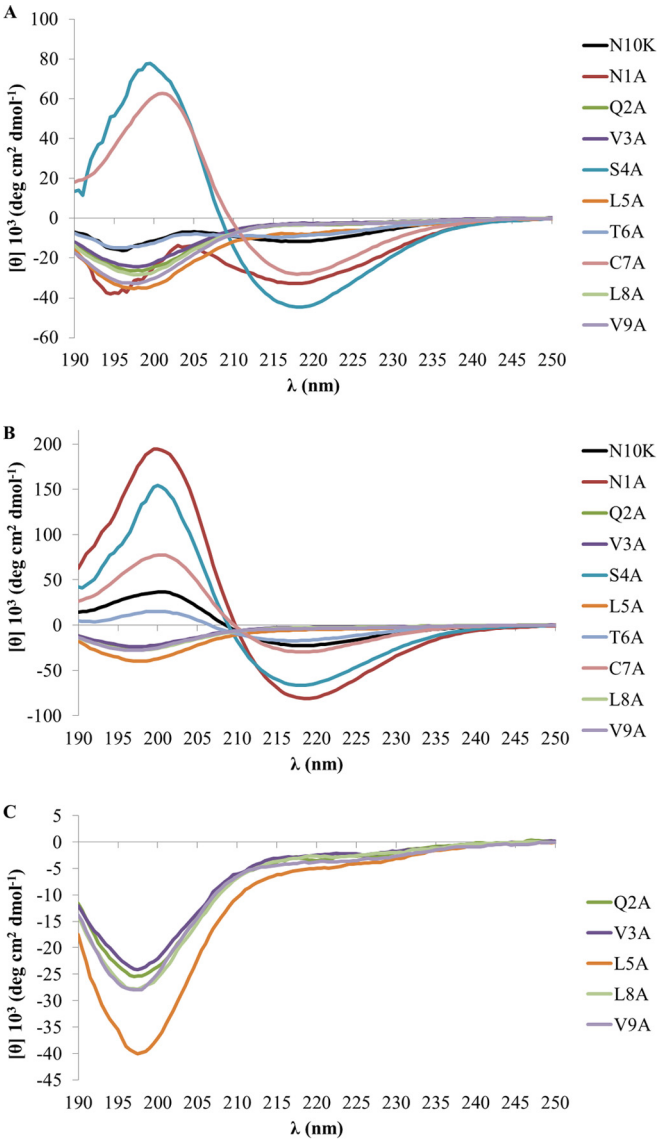

FIG 1 Far-UV CD spectra at 20°C of the N10K peptide and ASDs at 100 μM as a function of time. (A) Time zero; (B) 72 h after preparation of the starting aqueous solution (900 μM); (C) selected spectra from panel B plotted with an amplified vertical axis.

N1A ASD exhibited the highest increase in ellipticity, while the parental N10K peptide presented a CD spectrum with a lower intensity. As for the S4A and C7A ASDs, the CD spectrum showed an increase of the spectral intensity only for the S4A ASD (Fig. 1B). Finally, the CD spectra of the Q2A ASD and both V/A and L/A substitution peptides did not evidence any β-sheet formation, suggesting that they do not undergo any aggregation process, at least in the time interval tested (Fig. 1C).

Time kinetics of *C. albicans* killing. The N1A and L8A ASDs were both more active *in vitro* against *C. albicans* than the parental N10K peptide (Table 1) (9), in spite of showing opposite self-aggregation properties (Fig. 1). On the basis of these observations, the rates of killing of *C. albicans* over time by the N10K peptide and the N1A and L8A ASDs were determined with peptides at their minimal fungicidal concentration, 5 μg/ml for the N10K

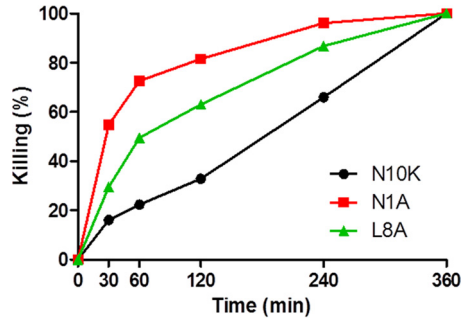

FIG 2 Time kinetics of *in vitro* activities of selected peptides against *Candida albicans* SC5314 cells. The activity is expressed as percent killing; data represent mean values from three independent experiments (variability ≤ 10%). Each experiment was performed in triplicate.

peptide and 2.5 μg/ml for the N1A and L8A ASDs. The N1A ASD demonstrated the faster candidacidal effect. In particular, the N1A ASD achieved 54.75% killing at 30 min and 72.61% killing at 60 min, in comparison to 16.09% and 22.40% for the N10K peptide, while the L8A ASD attained 29.55% and 49.51%, respectively (Fig. 2).

N1A ASD kinetics of dissociation. The N1A ASD, the derivative with the highest anti-*Candida* activity, also showed the highest degree of self-aggregation, as highlighted by the CD shape and by the intensity of the 200-nm band (Fig. 1B and Table 1). In addition, as demonstrated for another microbicidal killer peptide (11), for the N1A ASD, as well as for the N10K peptide and other active ASDs, the dimeric form turned out to be the active unit. In fact, these peptides, soon after solubilization under nonreducing conditions, did not show candidacidal activity, while candidacidal effect increased over time together with peptide dimerization (data not shown). Thus, N1A peptide conversion from the aggregated state to the active form was followed upon dilution and compared with the conversion, previously described, of the parental N10K peptide (9). In Fig. 3A and B are shown the CD spectra acquired using the N1A ASD in the self-aggregated form, 1 day or 3 days after preparation of the aqueous solution. Aliquots of the two preparations were diluted to 50 μM and the decrease of signal intensity at 200 nm was monitored over time. An isodichroic point at 211 nm was observed for both conditions, indicating a two-state nature of the dissociation transition. As assessed by plotting [θ] at 200 nm versus time, the N1A ASD is characterized by a dissociation rate 2-fold higher than that of the N10K peptide, with rate constants (k) of 14.9 and 25.6 min for 1-day-old solutions (Fig. 3C) and of 15.8 and 36.7 min for 3-day-old solutions (Fig. 3D), respectively.

Peptide-yeast cell interaction. Time-lapse confocal microscopy allowed us to investigate the dynamic process of peptide-yeast cells interaction. FITC-labeled N10K, N1A, and L8A peptides proved to enter living *C. albicans* SC5314 cells, gathering inside over time. This process, leading to cell death as shown by

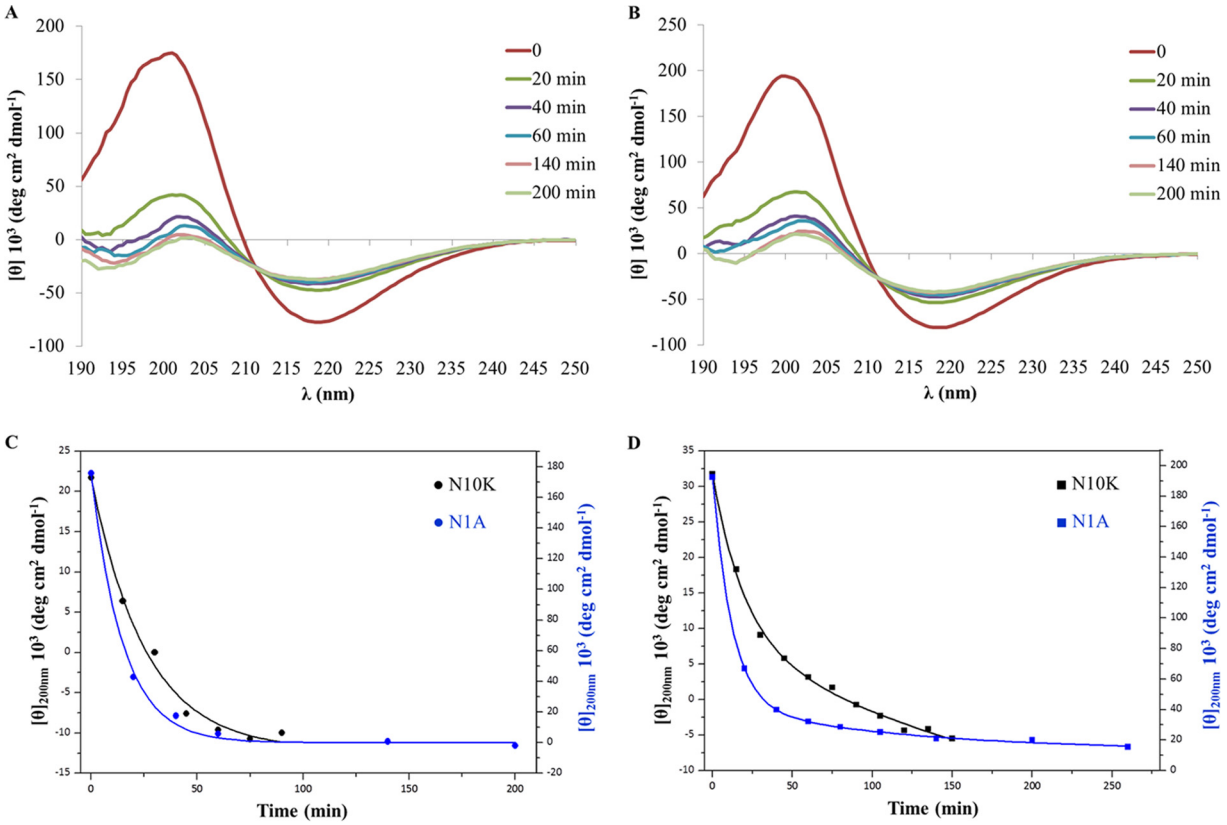

FIG 3 N1A ASD dissociation kinetics upon dilution. Far-UV CD spectra of a 50 μM concentration of the N1A ASD, prepared after 1 day (A) or 3 days (B) from the starting aqueous solution (900 μM), were acquired as a function of time. Shown also are plots of $[\theta]_{200}$ versus time for the N1A ASD and N10K parental peptide after 24 h (C) and 3 days (D).

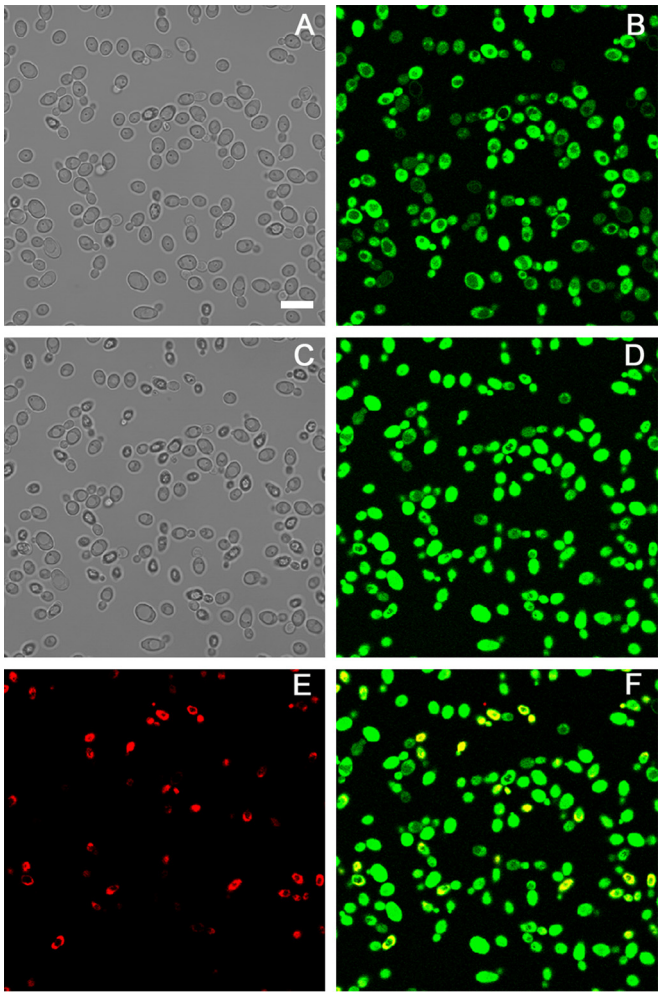

FIG 4 Internalization of the N1A ASD into *Candida albicans* SC5314 cells. Shown are confocal images of living yeast cells incubated in the presence of the fluorescein-labeled N1A ASD for 15 min (B) and 60 min (D). The same field is shown by light transmission images in panels A (15 min) and C (60 min). Bar = 10 μm. After 60 min, the N1A ASD is increasingly concentrated in yeast cells, and some of them are no longer viable as assessed by propidium iodide internalization (propidium iodide [E] and merge of panels D and E [F]).

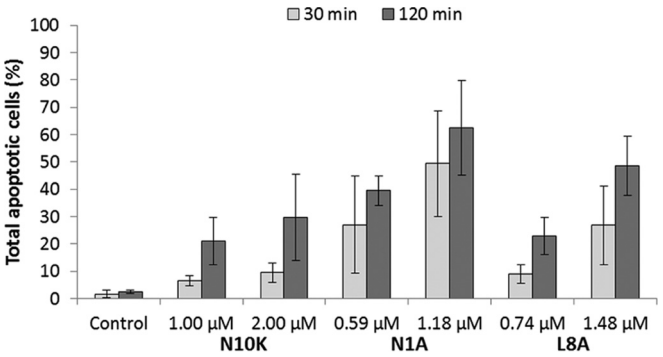

FIG 5 Apoptotic effects of the N10K peptide and selected ASDs in *Candida albicans* SC5314 cells. Phosphatidylserine externalization was analyzed by flow cytometry after 30 and 120 min of treatment with peptides at the EC_{50} and 2× EC_{50}. Data represent the means ± standard deviations from at least three independent experiments.

propidium iodide internalization, takes place at different rates for the three peptides. The N1A ASD entered more rapidly than the L8A ASD, while the N10K peptide took the longest time. As shown in Fig. 4, after 15 min of treatment, the FITC-labeled N1A ASD is inside all *C. albicans* cells. After 60 min, an increase of fluorescence is observed and some of the cells are already killed. With respect to the N10K peptide, the whole process took several hours. These results are consistent with the kinetics of yeast killing (see above). Interestingly, FITC-labeled V3A and C7A ASDs, which present a greatly reduced anti-*Candida* activity *in vitro*, proved to enter and gather inside living *C. albicans* cells in a similar way, although they were unable to cause cell death (see Fig. S1 in the supplemental material).

Induction of apoptosis and autophagy in *C. albicans* cells. Flow cytometry was used to assess if apoptosis and/or autophagy is induced in *C. albicans* SC5314 whole cells after treatment with the N1A, L8A, and N10K peptides. Under the experimental conditions adopted, all peptides were able to induce apoptosis, although to different extents. In particular, the percentage of apoptotic cells on the total gated cells turned out to be inversely related to the peptide EC_{50} and to be time and concentration dependent (Fig. 5). As an example, the apoptotic profile from a single assay performed on *C. albicans* cells treated for 30 and 120 min with the N1A ASD, in comparison with untreated cells (control), is shown in Fig. S2 in the supplemental material.

A change of the autophagy induction profile with respect to untreated cells was observed only after treatment with the N10K peptide (mean autophagy intensity, 31.4 ± 7.3 versus 9.9 ± 0.4). As an example, the results from a single assay performed on *C. albicans* cells treated with the N10K, N1A, and L8A peptides are shown in Fig. S3 in the supplemental material.

Self- and *C. albicans*-induced aggregation of the N1A and L8A ASDs. Electron micrographs of negatively stained N1A solutions at different concentrations, either freshly prepared in absence and in the presence of *C. albicans* cells (see Fig. S4 in the supplemental material) and even more after 7 months of storage (Fig. 6A), showed variable numbers of fibril-like structures that, based on previously observed CD spectra, are characterized by a β-sheet arrangement (9, 11). When *C. albicans* cells were added to the peptide solution, SEM images revealed gross N1A ASD aggregates surrounding the yeast cells (Fig. 6B).

In the case of the L8A ASD, instead, in agreement with the CD spectrum, typical of a random coil conformation both for a fresh preparation and for a 24-month-old preparation (Fig. 1 and 6C, respectively), electron micrographs evidenced the absence of any fibril-like structure (Fig. 6D). Nonetheless, when the 24-month-old preparation of the peptide was mixed with soluble β-glucans, its conformation changed immediately (Fig. 6C). Indeed, the CD difference spectrum of the L8A ASD in solution and upon addition of laminarin highlighted the presence of peptides arranged in β-sheet structures (Fig. 6C, inset). Based on this result, *C. albicans* cells were added to freshly prepared or 24-month-old L8A ASD solutions, and TEM and SEM showed the formation of a network of fibril-like structures on the surface of yeast cells (Fig. 6E and F; only the images of the 24-month-old preparation are shown).

A CFU assay performed on peptide-treated yeasts in comparison to control samples confirmed the candidacidal activities of the peptides under the experimental conditions adopted for SEM studies.

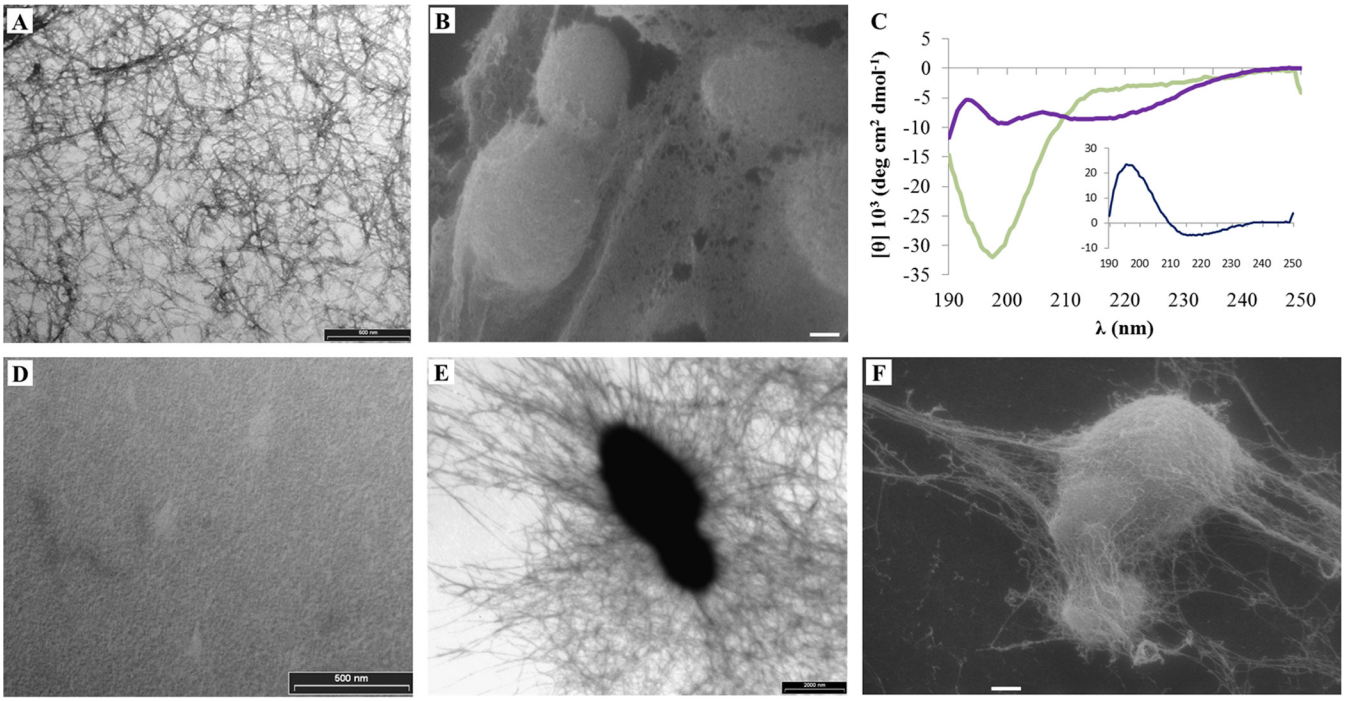

FIG 6 Aggregation of the N1A and L8A ASDs. (A) TEM image of a negatively stained 7-month-old solution of the N1A ASD showing self-aggregation in fibril-like structures. (B) SEM image of the same N1A ASD solution in the presence of *Candida albicans* SC5314 cells. (C) CD spectra of a 24-month-old solution of the L8A ASD in the absence (green line) or presence (purple line) of laminarin. The inset shows the difference spectrum between the L8A ASD in aqueous solution and in the presence of laminarin. (D) TEM image of a negatively stained 24-month-old solution of the L8A ASD showing no aggregation. (E and F) TEM and SEM images of the same peptide in the presence of *C. albicans* cells. TEM images bars = 500 nm (A and D) and 2,000 nm (E). SEM image bars = 1 μm.

Role of laminarin in the self-aggregation process. Previous studies by CD spectroscopy revealed that in aqueous solution, the N10K peptide dimerizes, acquiring a β-sheet secondary structure, and that in few hours, the dimeric units aggregate in ordered β-sheet fibril-like structures (9).

The thermal stability of those aggregates, starting from a 7-day-old aggregated N10K peptide, was studied by CD spectroscopy, and the results are shown in Fig. 7. At 20°C, the N10K peptide presents a CD spectrum with the positive band around 200 nm and the negative one at 218 nm with an intensity ratio of 2:1, typical of peptides in a β-sheet conformation. Along with the temperature increase from 20°C to 90°C, the intensity of the two bands decreased gradually (data not shown) until the CD spectrum acquired the shape typical of peptides in a disordered conformation. In contrast, in the presence of laminarin, the β-sheet conformation is preserved up to 90°C, although with a slight decrease in the intensity of the dichroic bands. Upon cooling to 20°C, in the absence of laminarin the N10K peptide did not recover any ordered secondary structure. Instead, in the presence of laminarin the peptide retained its conformational organization throughout the thermal cycle (Fig. 7).

***In vivo* toxicity and therapeutic activity.** Toxicity against the host and therapeutic activity against *C. albicans* infection were evaluated for the N1A and L8A ASDs in *G. mellonella* larvae, in comparison with those of the N10K peptide, whose therapeutic activity in consolidated models of murine systemic and mucosal candidiasis has been already described (9).

We verified that under the adopted conditions, there was no significant difference in survival between larvae inoculated with saline (control group) and with the peptides (see Fig. S5 in the supplemental material), showing that the peptides were not toxic in this experimental model.

The therapeutic effects of the three peptides were evaluated in larvae infected with *C. albicans* SC5314. A single injection (10 μl) of both the N10K and N1A peptides (450 μM) led to a significant

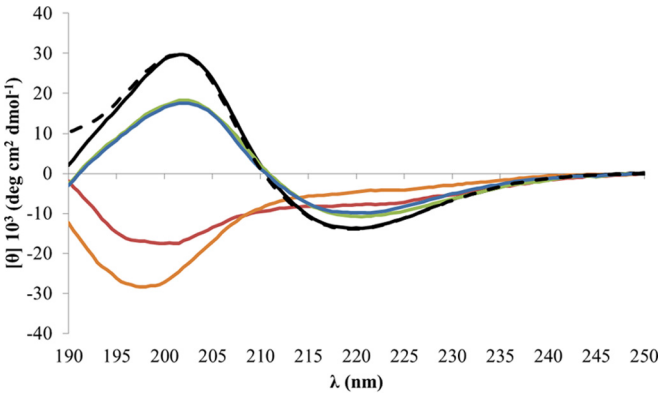

FIG 7 N10K peptide thermal disaggregation. CD spectra of a 100 μM concentration of the N10K peptide, prepared from a starting aqueous solution stored for 7 days at 4°C, were acquired at 20°C (in the absence [dashed black line] and presence [continuous black line]of 500 μM laminarin), after heating at 90°C (in the absence [red line] and presence [green line] of laminarin), and after cooling back at 20°C (in the absence [orange line] and presence [blue line] of laminarin). Temperature increase and decrease were 1°C/min up to 90°C and the reverse.

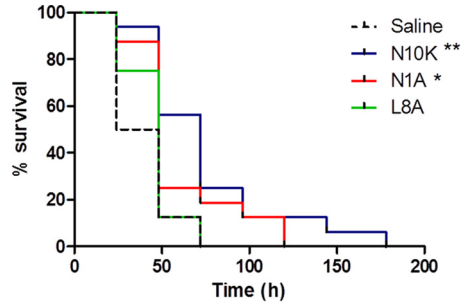

FIG 8 Therapeutic activity of selected peptides. Groups of 16 *Galleria mellonella* larvae were infected with 5×10^5 cells of *Candida albicans* SC5314 and treated with peptides (10 μmol/kg; single injection of 10 μl) or saline solution (control group). The survival curves of N10K peptide- and N1A ASD-treated larvae were significantly different from that for the control group, as assessed by Mantel-Cox log rank test (**, $P < 0.01$; *, $P < 0.05$).

increase in survival of larvae in comparison to that of infected animals inoculated with saline (P values of <0.01 and <0.05, respectively), with the N10K peptide being more effective than the N1A ASD. In contrast, the survival of larvae treated with the L8A ASD did not differ from the survival of larvae in the control group (Fig. 8).

DISCUSSION

The N10K synthetic peptide, whose sequence is present in the human IgG1 constant region, proved to be fungicidal *in vitro* against fungal pathogens, including multidrug-resistant strains, and to exert a therapeutic effect against murine systemic and mucosal experimental *Candida* infection (9). We postulated that the therapeutic activity of the N10K peptide had to be related to its ability to form dimers, considered to be the peptide active unit. More than that, we envisaged that self-aggregation is a process that protects the peptide from protease degradation, thus ensuring a prolonged *in vivo* lifetime. This phenomenon has been previously observed and described as a novel paradigm of targeted autodelivery for a killer peptide (11, 14).

As proposed in the early 1950s (15–17), alternation of hydrophobic and polar amino acids, as in the N10K peptide, promotes the acquisition of a β-sheet structure and the formation of large self-assembling aggregates or filaments, mediated by hydrogen bonds and hydrophobic, electrostatic, van der Waals, and aromatic π-π interactions (18, 19), in which the β-sheet organization is preserved. Indeed, N10K peptide aggregation in fibril-like structures was confirmed by TEM studies.

Previous studies highlighted that Ala scanning of the N10K peptide produced peptides characterized by specific *in vitro* fungicidal activities (9). Using that family of peptides, we sought to devise a molecular model that correlates the self-assembly propensity and structural stability of the aggregates they form with *in vitro* candidacidal activity and *in vivo* therapeutic efficacy.

While the N1A ASD exhibits an enhanced propensity to self-assemble compared to parental N10K peptide, the Gln/Ala, Val/Ala, and Leu/Ala changes produce the opposite effect. As for the K10A ASD, because of the loss of the only positively charged residue, it turns out to be water insoluble.

The disulfide bond near the middle of the amphipathic peptide sequence leads to dimer stabilization and appears to be critical for dimer aggregation. In fact, the behavior of the C7A ASD, which immediately acquires a β-conformation but does not form fibril-like structures, may be explained by the absence of the sulfur bridge that allows a conformational freedom of the dimeric units not compatible with fibril formation (20).

The comparative analysis of the kinetics of *C. albicans* cell killing by the most active peptides *in vitro* showed that the N1A ASD exhibits a higher rate of killing than the N10K peptide. Consistent with these results, we found that N1A derivative aggregates diluted in water lose their structural organization twice as fast as the N10K peptide, thus supporting the hypothesis that the release of the dimeric unit is an essential step for peptide biologic activity.

All the investigated peptides proved to enter yeast cells regardless of their biological activities. Amino acid substitutions which turned out to have a negative impact on the candidacidal property of the peptides did not affect their binding to yeast cells or internalization. The N10K peptide and the ASDs endowed with candidacidal activity were able to induce apoptosis, although, most likely, this was not the sole cause of death, as deduced by the reduction of the total number of gated cells already found after 30 min of treatment (see Fig. S2 in the supplemental material; note that nonapoptotic dead cells are not included in the number of gated cells, being below the threshold settings based on the size index). Interestingly, only the N10K peptide can enhance cell autophagy. Autophagy is generally considered a survival mechanism or a degradative process that is activated as a response to starvation; organelles can be eliminated by nonselective or selective autophagy, the latter occurring in response to organelle damage or dysfunction (21). At this stage, we have no explanation for this result. We can only accept the evidence that N10K peptide-*Candida* cell interaction is unique among the members of this peptide family.

The N1A and L8A ASDs exhibited higher *in vitro* candidacidal activities than the parental N10K peptide. While for the N1A peptide this observation is justified by its pronounced propensity to form β-sheet structures and self-aggregate in water, at first glance it appears inconsistent for the L8A ASD, which persists in a random coil conformation even after several months in water solution. However, CD, TEM, and SEM studies demonstrated that the L8A ASD is capable of forming β-structures when interacting with β-glucans, either soluble or present on yeast cell wall, thus suggesting that the glucans act as a template on which the dimers can bind and assemble in fibril-like structures.

Indeed, the possibility for the peptides to interact with β-glucans appears essential also to stabilize the fibril-like aggregates, even under extreme conditions as confirmed by the temperature-dependent dissociation of N10K peptide aggregates in the presence of laminarin. Interestingly, at least under the adopted experimental conditions, at high temperature, in the absence of laminarin, N10K peptide disaggregation is complete and single dimers are not able to reassemble (Fig. 7).

Overall, we can hypothesize that the aggregates *in vitro* are involved in the interaction with the cell surface and that from those aggregates, because of the dilution effect due to the distribution on the cell surface, the dimeric active units are released and penetrate the cell.

If, on the basis of this molecular model, we consider the therapeutic efficacy *in vivo* of these peptides, the fact that the N1A and N10K peptides, unlike the L8A ASD, are protective in an *in vivo* model of *Candida* infection confirms that the ability to self-assem-

ble in the absence of β-glucans is important for *in vivo* candidacidal activity since it protects the peptides against proteases.

The relevance of the aggregation property of these peptides in modulating their *in vitro* and *in vivo* candidacidal activities is also exemplified by the observation that while *in vitro* the N1A ASD is more effective than the N10K peptide, *in vivo* the situation reverts. The enhanced resistance of N10K peptide fibrils to disaggregate allows a more prolonged resistance of this peptide to the action of proteolytic enzymes, thus favoring the binding to a larger number of yeast cells.

In summary, the investigated candidacidal peptides interact with the yeast surface and are able, to various extents, to penetrate inside the cell and to activate apoptosis. It is worth noting, however, that this study highlights three relevant structural and functional features: (i) some residues in the peptide primary sequence play a critical role in favoring self-aggregation (Table 1), (ii) the peptides with an enhanced killing and therapeutic activity are those able to form fibril-like aggregates, and (iii) the rate of formation and stability of the fibril-like aggregates play a dual role in modulating the candidacidal activity *in vitro* and influencing the therapeutic efficiency *in vivo*.

Although the mechanism of action of these peptides has yet to be clearly understood, these results provide the basis to design new and more effective antimicrobial peptides.

ACKNOWLEDGMENTS

We thank Silvana Belletti and Davide Dallatana for technical assistance in confocal microscopy and SEM studies and C.I.M. Laboratory, Technopole Parma, University of Parma, for the use of the spectropolarimeter.

L.G. acknowledges financial support from MIUR Italy through the FIRB-Futuro in ricerca (RBFR136GFF) program.

FUNDING INFORMATION

This research received no specific grant from any funding agency in the public, commercial, or not-for-profit sectors. L.G. acknowledges financial support from MIUR Italy through the "FIRB-Futuro in ricerca" (RBFR136GFF) program.

REFERENCES

1. **Mandal SM, Roy A, Ghosh AK, Hazra TK, Basak A, Franco OL.** 2014. Challenges and future prospects of antibiotic therapy: from peptides to phages utilization. Front Pharmacol **5:**105.
2. **Magliani W, Conti S, Cunha RL, Travassos LR, Polonelli L.** 2009. Antibodies as crypts of antiinfective and antitumor peptides. Curr Med Chem **16:**2305–2323. http://dx.doi.org/10.2174/092986709788453104.
3. **Magliani W, Conti S, Giovati L, Zanello PP, Sperindè M, Ciociola T, Polonelli L.** 2012. Antibody peptide based antifungal immunotherapy. Front Microbiol **3:**190.
4. **Polonelli L, Pontón J, Elguezabal N, Moragues MD, Casoli C, Pilotti E, Ronzi P, Dobroff AS, Rodrigues EG, Juliano MA, Maffei DL, Magliani W, Conti S, Travassos LR.** 2008. Antibody complementarity-determining regions (CDRs) can display differential antimicrobial, antiviral and antitumor activities. PLoS One **3:**e2371. http://dx.doi.org/10.1371/journal.pone.0002371.
5. **Gabrielli E, Pericolini E, Cenci E, Ortelli F, Magliani W, Ciociola T, Bistoni F, Conti S, Vecchiarelli A, Polonelli L.** 2009. Antibody complementarity-determining regions (CDRs): a bridge between adaptive and innate immunity. PLoS One **4:**e8187. http://dx.doi.org/10.1371/journal.pone.0008187.
6. **Dobroff AS, Rodrigues EG, Juliano MA, Friaça DM, Nakayasu ES, Almeida IC, Mortara RA, Jacysyn JF, Amarante-Mendes GP, Magliani W, Conti S, Polonelli L, Travassos LR.** 2010. Differential antitumor effects of IgG and IgM monoclonal antibodies and their synthetic complementarity-determining regions directed to new targets of B16F10-Nex2 melanoma cells. Transl Oncol **3:**204–217. http://dx.doi.org/10.1593/tlo.09316.
7. **Arruda DC, Santos LCP, Melo FM, Pereira FV, Figueiredo CR, Matsuo AL, Mortara RA, Juliano MA, Rodrigues EG, Dobroff AS, Polonelli L, Travassos LR.** 2012. β-Actin-binding complementarity-determining region 2 of variable heavy chain from monoclonal antibody C7 induces apoptosis in several human tumor cells and is protective against metastatic melanoma. J Biol Chem **287:**14912–14922. http://dx.doi.org/10.1074/jbc.M111.322362.
8. **Figueiredo CR, Matsuo AL, Massaoka MH, Polonelli L, Travassos LR.** 2014. Anti-tumor activities of peptides corresponding to conserved complementary determining regions from different immunoglobulins. Peptides **59:**14–19. http://dx.doi.org/10.1016/j.peptides.2014.06.007.
9. **Polonelli L, Ciociola T, Magliani W, Zanello PP, D'Adda T, Galati S, De Bernardis F, Arancia S, Gabrielli E, Pericolini E, Vecchiarelli A, Arruda DC, Pinto MR, Travassos LR, Pertinhez TA, Spisni A, Conti S.** 2012. Peptides of the constant region of antibodies display fungicidal activity. PLoS One **7:**e34105. http://dx.doi.org/10.1371/journal.pone.0034105.
10. **Gabrielli E, Pericolini E, Cenci E, Monari C, Magliani W, Ciociola T, Conti S, Gatti R, Bistoni F, Polonelli L, Vecchiarelli A.** 2012. Antibody constant region peptides can display immunomodulatory activity through activation of the Dectin-1 signalling pathway. PLoS One **7:**e43972. http://dx.doi.org/10.1371/journal.pone.0043972.
11. **Pertinhez TA, Conti S, Ferrari E, Magliani W, Spisni A, Polonelli L.** 2009. Reversible self-assembly: a key feature for a new class of autodelivering therapeutic peptides. Mol Pharmaceut **6:**1036–1039. http://dx.doi.org/10.1021/mp900024z.
12. **Gatti R, Orlandini G, Uggeri J, Belletti S, Galli C, Raspanti M, Scandroglio R, Guizzardi S.** 2008. Analysis of living cells grown on different titanium surfaces by time-lapse confocal microscopy. Micron **39:**137–143. http://dx.doi.org/10.1016/j.micron.2006.11.009.
13. **Desbois AP, Coote PJ.** 2012. Utility of greater wax moth larva (*Galleria mellonella*) for evaluating the toxicity and efficacy of new antimicrobial agents. Adv Appl Microbiol **78:**25–53. http://dx.doi.org/10.1016/B978-0-12-394805-2.00002-6.
14. **Magliani W, Conti S, Ciociola T, Giovati L, Zanello PP, Pertinhez T, Spisni A, Polonelli L.** 2011. Killer peptide: a novel paradigm of antimicrobial, antiviral and immunomodulatory auto-delivering drugs. Future Med Chem **3:**1209–1231. http://dx.doi.org/10.4155/fmc.11.71.
15. **Pauling L, Corey RB.** 1951. Configurations of polypeptide chains with favored orientations around single bonds: two new pleated sheets. Proc Natl Acad Sci U S A **37:**729–740. http://dx.doi.org/10.1073/pnas.37.11.729.
16. **Pauling L, Corey RB.** 1953. Two rippled-sheet configurations of polypeptide chains, and a note about the pleated sheets. Proc Natl Acad Sci U S A **39:**253–256. http://dx.doi.org/10.1073/pnas.39.4.253.
17. **Marsh RE, Corey RB, Pauling L.** 1955. An investigation of the structure of silk fibroin. Biochim Biophys Acta **16:**1–34. http://dx.doi.org/10.1016/0006-3002(55)90178-5.
18. **Bemporad F, Calloni G, Campioni S, Plakoutsi G, Taddei N, Chiti F.** 2006. Sequence and structural determinants of amyloid fibril formation. Acc Chem Res **39:**620–627. http://dx.doi.org/10.1021/ar050067x.
19. **Hamley IW.** 2007. Peptide fibrillization. Angew Chem Int Ed Engl **46:**8128–8147. http://dx.doi.org/10.1002/anie.200700861.
20. **Larsen TH, Branco MC, Rajagopal K, Schneider JP, Furst EM.** 2009. Sequence-dependent gelation kinetics of beta-hairpin peptide hydrogels. Macromolecules **42:**8443–8450. http://dx.doi.org/10.1021/ma901423n.
21. **Reggiori F, Klionsky DJ.** 2013. Autophagic processes in yeast: mechanism, machinery and regulation. Genetics **194:**341–361. http://dx.doi.org/10.1534/genetics.112.149013.